US 20250019839A1

(19) **United States**
(12) **Patent Application Publication**
Wang et al.
(10) **Pub. No.: US 2025/0019839 A1**
(43) **Pub. Date: Jan. 16, 2025**

(54) **SUBSTANTIAL LIFETIME ENHANCEMENT OF SI-BASED PHOTOANODES ENABLED BY AMORPHOUS TIO2 COATING WITH IMPROVED STOICHIOMETRY**

(71) Applicants: **Wisconsin Alumni Research Foundation**, Madison, WI (US); **Ohio State Innovation Foundation**, Columbus, OH (US)

(72) Inventors: **Xudong Wang**, Middleton, WI (US); **Yutao Dong**, Madison, WI (US); **Dane Morgan**, Middleton, WI (US); **Jun Meng**, Madison, WI (US); **Jinwoo Hwang**, Cincinnati, OH (US); **Mehrdad Abbasi Gharacheh**, Portland, OR (US)

(21) Appl. No.: **18/747,661**

(22) Filed: **Jun. 19, 2024**

Related U.S. Application Data

(60) Provisional application No. 63/526,515, filed on Jul. 13, 2023.

Publication Classification

(51) **Int. Cl.**
C25B 11/049 (2006.01)
C25B 11/059 (2006.01)
C25B 11/087 (2006.01)

(52) **U.S. Cl.**
CPC ***C25B 11/049*** (2021.01); ***C25B 11/059*** (2021.01); ***C25B 11/087*** (2021.01)

(57) **ABSTRACT**

A post-ALD in-situ water treatment procedure is used to remove the ligand residues in amorphous TiO_2 films coated on photoanode material to improve the film stoichiometry without introducing any additional crystallization. The processed amorphous TiO_2 film showed drastically improved chemical stability, and thereby substantially elongated the lifetime of silicon-based photoanodes in alkaline electrolyte.

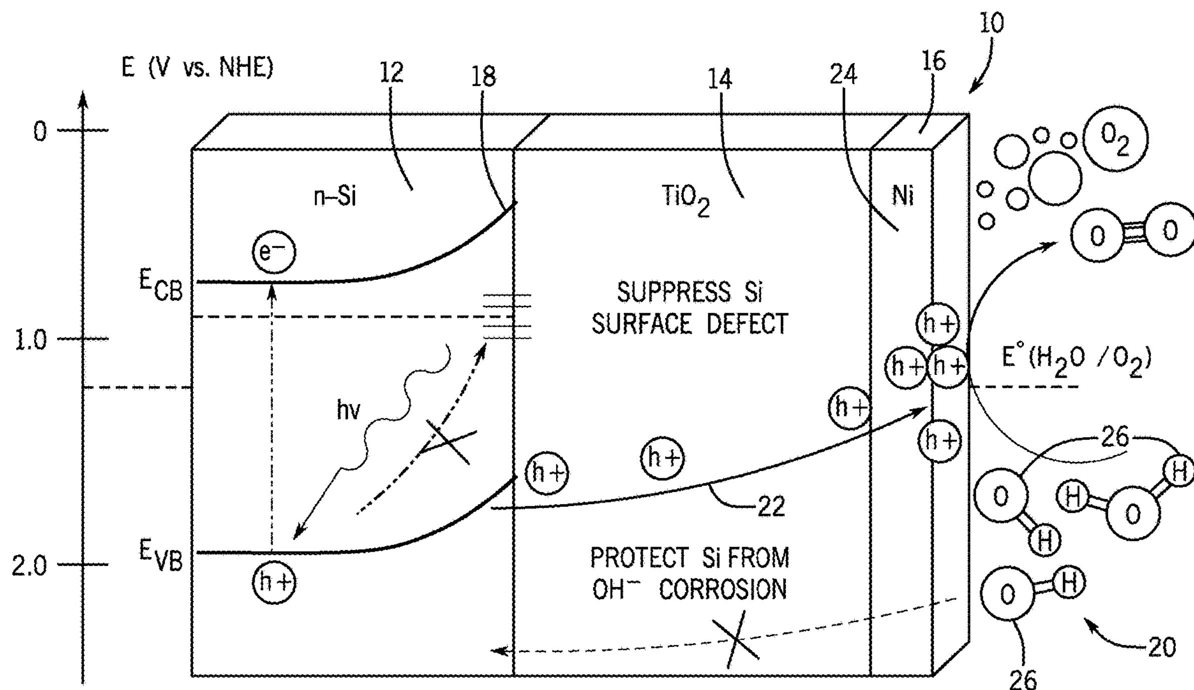

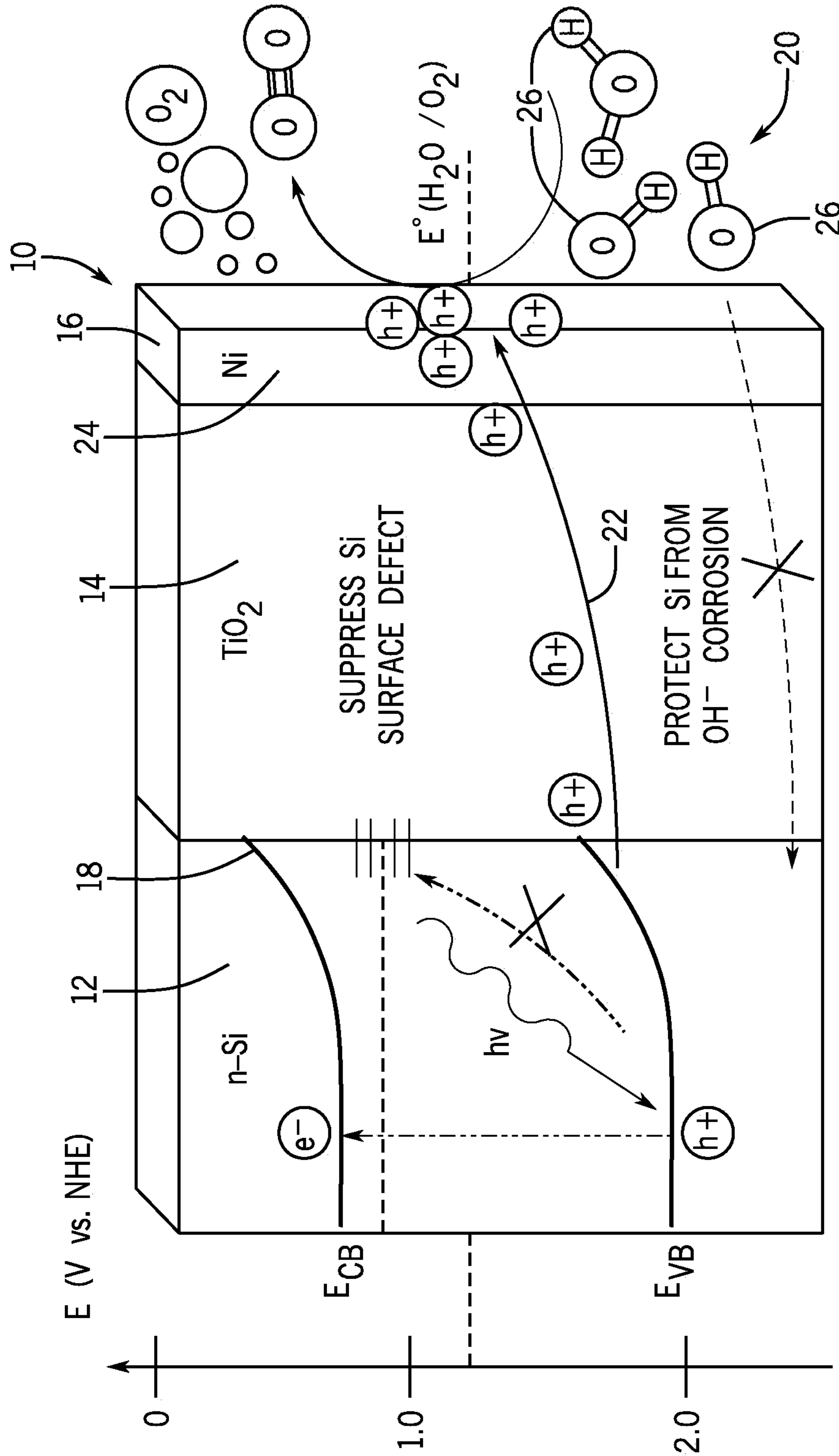

FIG. 1

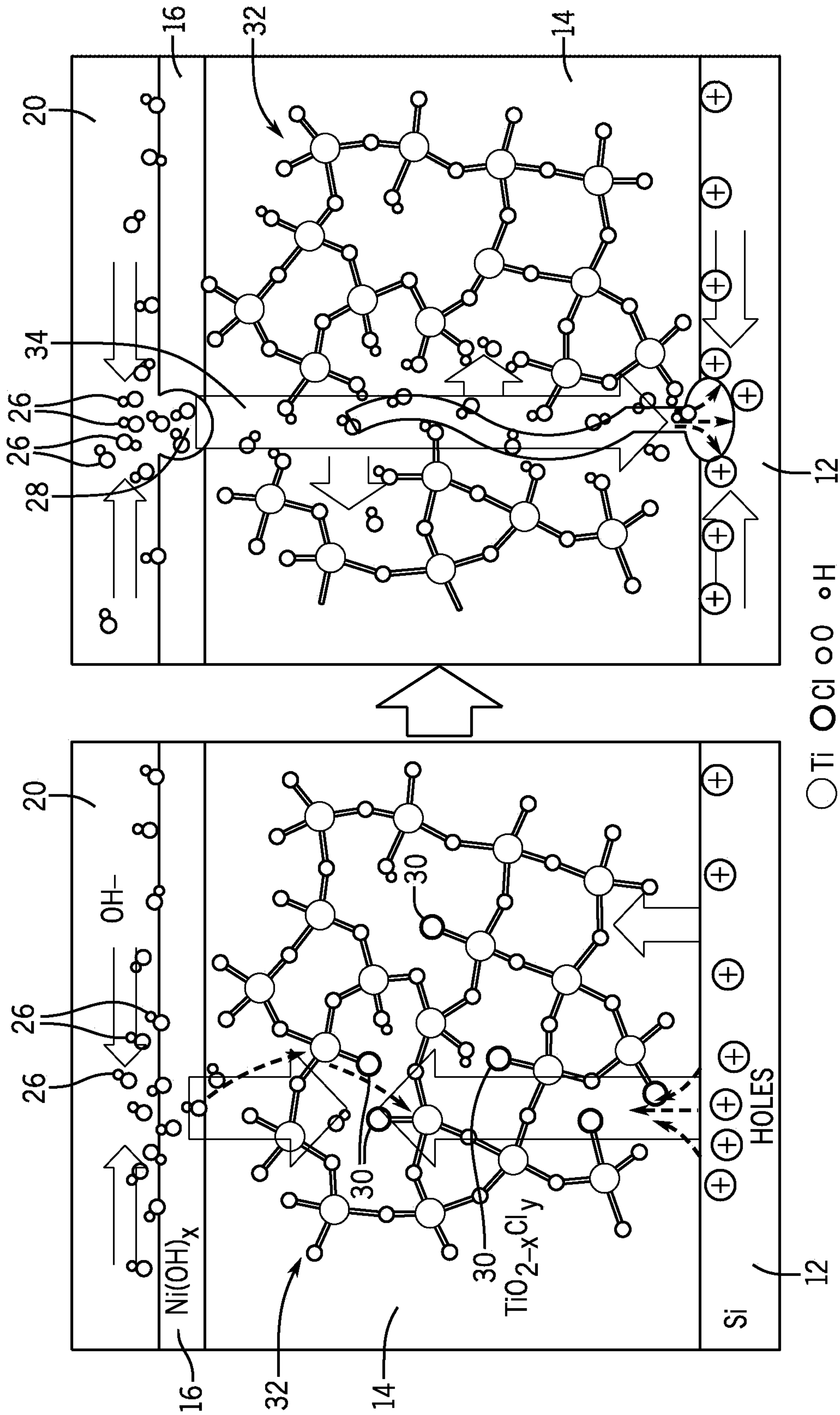

FIG. 2

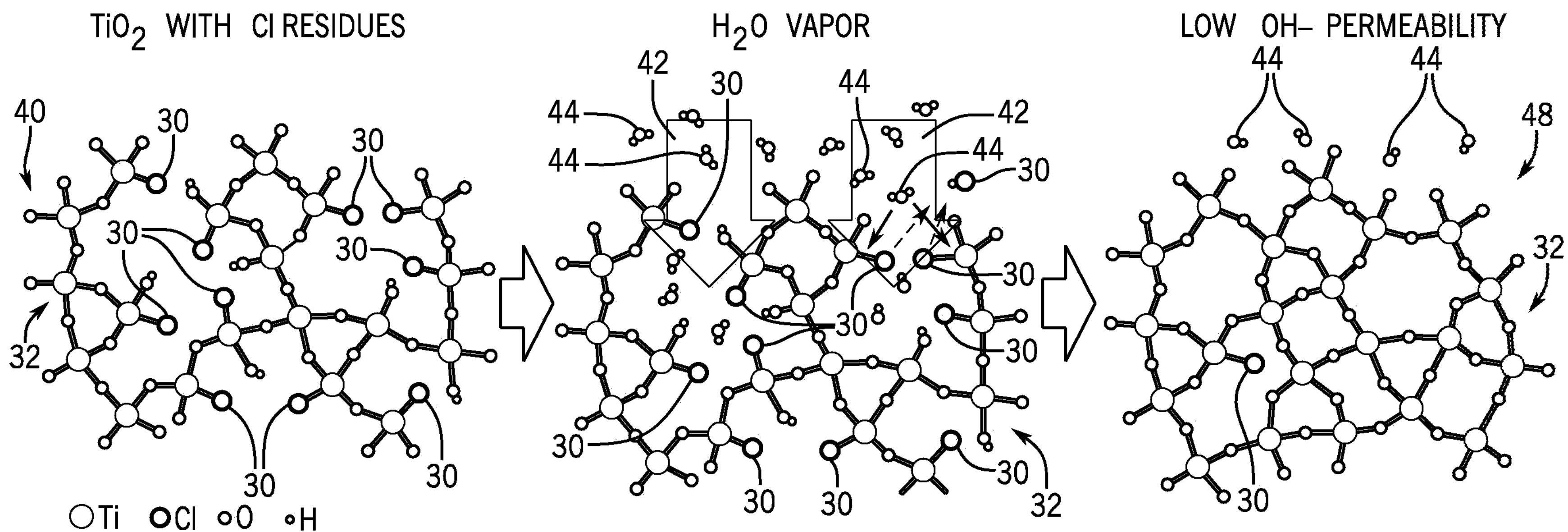

FIG. 3

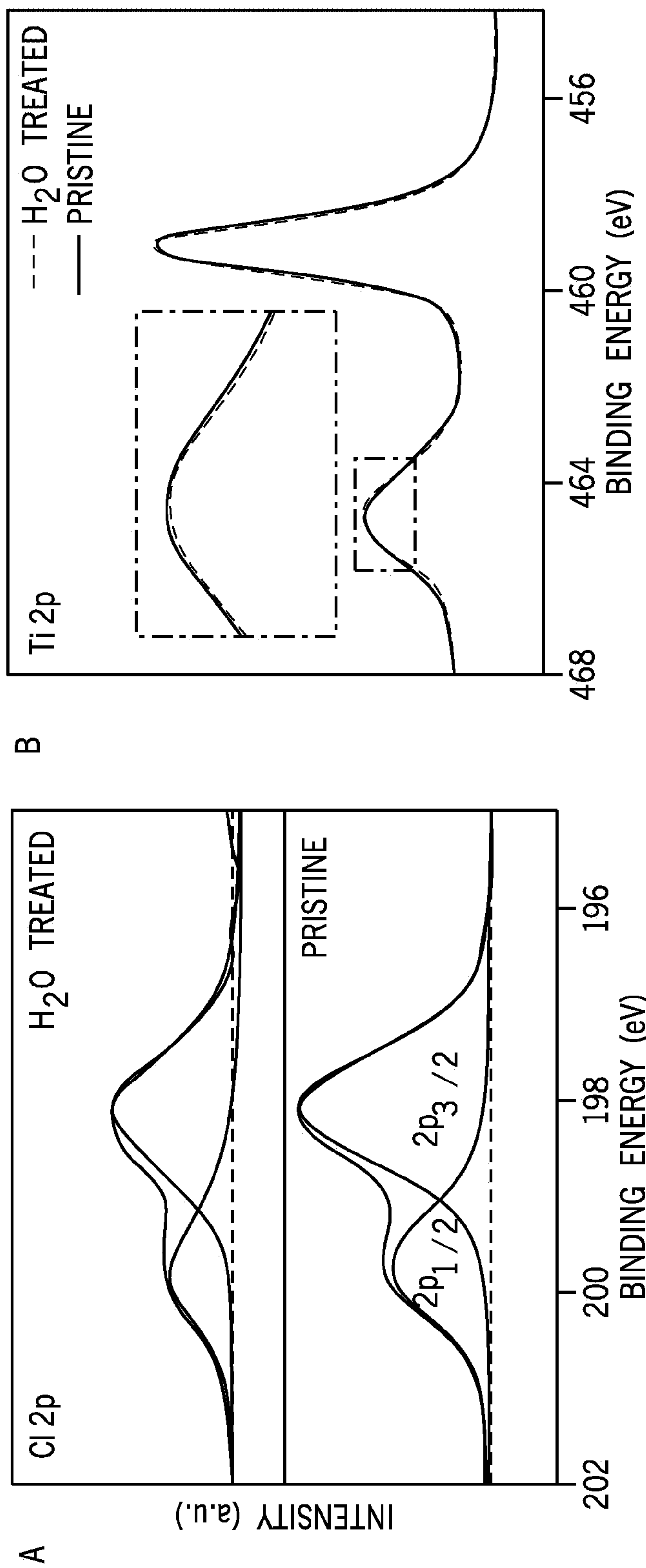

FIG. 4

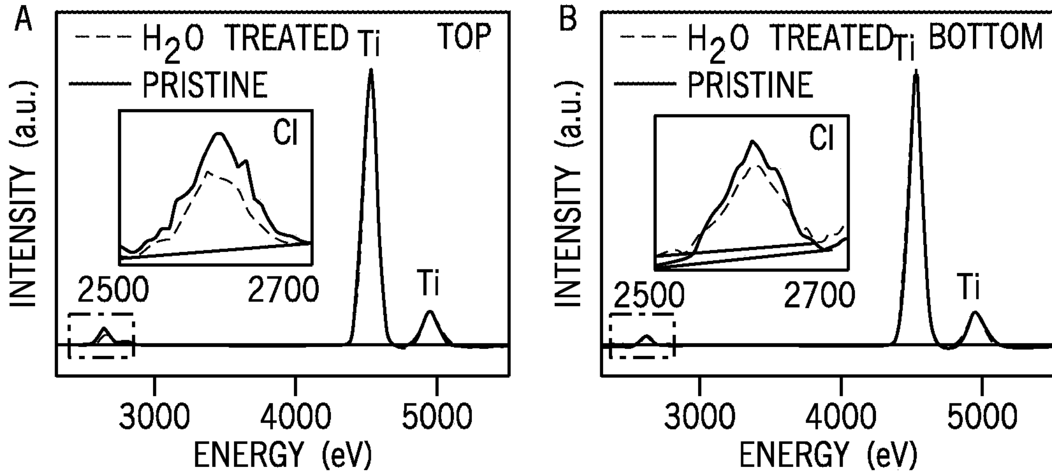

FIG. 5

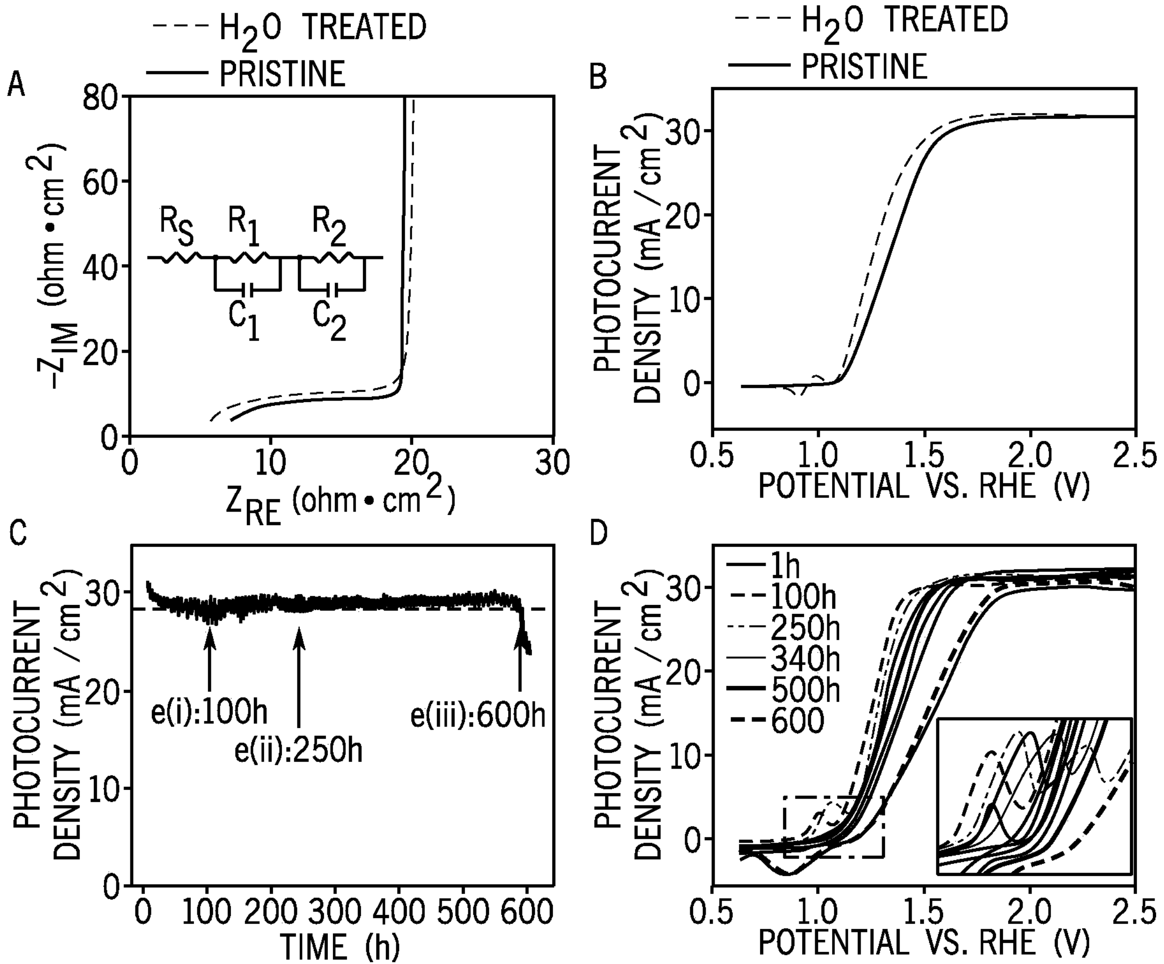

FIG. 6

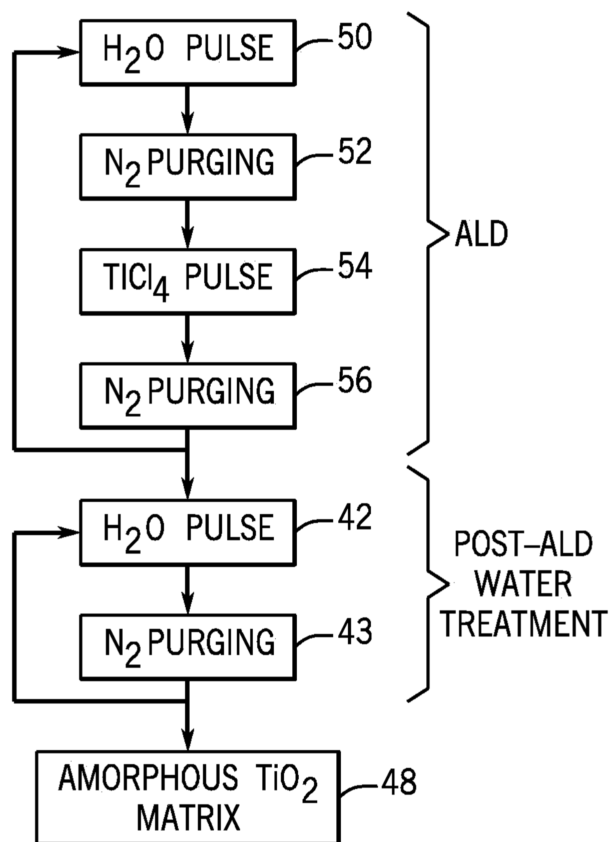

FIG. 7

SUBSTANTIAL LIFETIME ENHANCEMENT OF SI-BASED PHOTOANODES ENABLED BY AMORPHOUS TIO2 COATING WITH IMPROVED STOICHIOMETRY

CROSS REFERENCE TO RELATED APPLICATION

[0001] This application claims the benefit of U.S. provisional application 63/526,515 filed Jul. 13, 2023 and incorporated by reference.

STATEMENT REGARDING FEDERALLY SPONSORED RESEARCH OR DEVELOPMENT

[0002] This invention was made with government support under DE-SC0020283 awarded by the US Department of Energy. The government has certain rights in the invention.

BACKGROUND OF THE INVENTION

[0003] The present invention relates to photoelectrodes, and more particularly, to photoelectrochemical cells used to extract electrical energy from light, including sunlight.

[0004] Renewable energy sources are an important solution to counteract the growing need to replace fossil fuels, responsible for the rise in global temperature. Hydrogen energy is a chemical bond energy that is converted into electricity by a fuel cell which is an electrochemical converter energy device. Favorably, pure water is the only byproduct of hydrogen energy source.

[0005] Supply of hydrogen molecules is limited because they are not found naturally as gas form but are found naturally bound to other elements such as oxygen in water molecules and carbon as hydrocarbon molecules. Although hydrogen is mostly produced through natural gas reforming of hydrocarbons, i.e., methane (CH_4), extracting hydrogen from water molecules (H_2O) is desired because water molecules are abundant and do not release harmful byproducts such as CO_2.

[0006] Photoelectrochemical (PEC) water splitting is considered a promising approach to hydrogen fuel generation. In PEC water splitting, hydrogen is produced from water using light such as sunlight and specialized semiconductors called photoelectrochemical materials, which use the light energy to directly dissociate water molecules into hydrogen and oxygen. The photoelectrochemical materials, such as silicon, convert solar energy directly to chemical energy in the form of hydrogen. The semiconductor materials used in the PEC process are similar to those used in photovoltaic solar electricity generation, but for PEC applications the semiconductor is immersed in a water-based electrolyte, where sunlight energizes the water-splitting process. PEC reactors can be constructed in panel form (like photovoltaic panels) as electrode systems or as slurry-based particle systems.

[0007] The U.S. Department of Energy (DOE) has set PEC water-splitting commercialization targets of a solar-to-hydrogen efficiency of approximately 25% and an electrode replacement lifetime of approximately 10 years of operation under diurnal cycles and approximately 5 years of actual hydrogen production. The minimal industrial requirement lifetime is about 30,000 hours. Therefore, PEC devices require not only high solar to hydrogen conversion efficiency but also high chemical stability in strong acidic or alkaline electrolytes for long-term operation.

[0008] Silicon (Si) is a commonly used photoanode material that delivers high energy conversion efficiency because of its appropriate band structure and excellent charge mobility. However, Si exhibits a very short lifetime of only a few hours. The solar-to-hydrogen conversion efficiency of a Si photoelectrode is suppressed by overpotential, high reflectance, and its instability in liquid electrolytes, i.e., rapid corrosion or dissolution in alkaline electrolytes. To improve its lifetime, a prevailing strategy is to protect the reactive photoanode surfaces with a conformal and pinhole-free inert oxide coating by atomic layer deposition (ALD). While both crystalline and amorphous ALD oxide films have been applied for surface protection, amorphous ALD coatings are more commonly used because of their excellent uniformity and conformality.

[0009] Titanium dioxide (TiO_2) has been considered a highly promising protection layer and amorphous ALD coating to achieve high chemical stability for PEC water splitting devices, especially for Si-based monolithic photovoltaic electrochemical (PV-EC) systems. The highest reported lifetime of Si-based photoanode is achieved by amorphous TiO_2 coating at the level of 500 hours, which however, is still far below the minimal industrial requirement (~30,000 hours).

[0010] It is believed that there is a trade-off relationship between activity and stability in these devices due to the high charge transport barrier at the Si/TiO_2 interface and the high ohmic loss in TiO_2 films which hinder the device performance, especially when a thick TiO_2 protection layer (preferred to enhance the chemical stability in the electrolyte) is used. Therefore, the protection performance of TiO_2 protection layer is primarily tuned by adjusting protection layer thickness.

SUMMARY OF THE INVENTION

[0011] The present inventors have discovered the existence of highly conductive intermediates in amorphous TiO_2 thin films. These intermediates (e.g., atom clusters, amorphous particles, and non-bulk crystal-like structures) are kinetically trapped structures between the amorphous and the crystalline phases. These intermediates have a non-bulk crystal-like structure and induce significant inhomogeneity in the amorphous TiO_2 thin film. These impurities may substantially change the amorphous TiO_2 thin film's properties, such as electronic and ionic transport properties, mechanical stability, and chemical reactivity.

[0012] Structural inhomogeneity in the amorphous TiO_2 thin film (e.g., imbedded intermediate phases) induce highly localized current through the amorphous film, raises the local concentration of hydroxyls, and facilitates pinhole formation through the amorphous matrix. These findings have been described in the inventors' publication, Yu, Yanhao, et al. "Metastable intermediates in amorphous titanium oxide: A hidden role leading to ultra-stable photoanode protection." *Nano Letters* 18.8 (2018): 5335-5342, and is hereby incorporated by reference.

[0013] Therefore, a strategy to improve the protection longevity is to maximize electrical homogeneity of the amorphous thin film by suppressing the formation of intermediates. Thus, a low-temperature, crystalline-free, amorphous thin film is preferable for achieving a longer lifetime.

[0014] Further, in amorphous TiO_2 thin films deposited by ALD processes at low temperature, residual ligands are inevitable. Therefore, the unreacted precursor ligands and

byproducts are another issue associated with low temperature ALD processes. The present inventors have expanded their prior research by further identifying the detrimental role of the residual chloride (Cl) ligands in amorphous TiO_2 thin films to the PEC protection lifetime.

[0015] The present invention provides a post-ALD in-situ water treatment procedure to at least partially remove the Cl ligand residues and improve the film stoichiometry without introducing any additional crystallization. The processed amorphous TiO_2 thin film showed drastically improved chemical stability, and thereby substantially elongated the lifetime of Si photoanodes in the alkaline electrolyte.

[0016] Specifically, the present invention provides a method of removing precursor ligands and byproducts in a photoelectrode, the method comprising: (a) performing an atomic layer deposition of an oxide onto a photoanode material including the steps of: pulsing oxygen precursors onto a photoanode material surface; purging the photoanode material surface with an inert gas; pulsing metal precursors onto the photoanode material surface; and purging the photoanode material surface with the inert gas to deposit a thin film of oxide onto the photoanode material surface to produce a thin film matrix; (b) performing a water treatment of the thin film matrix including the steps of: pulsing an oxygen precursor such as water onto the thin film matrix; and purging the thin film matrix with an inert gas to reduce a ratio of remaining precursor ligand to oxide from the thin film matrix.

[0017] It is thus a feature of at least one embodiment of the present invention to remove unreacted precursor ligands from the thin film matrix which are responsible for introducing a more permeable amorphous lattice allowing a faster reaction between the OH^- of the alkaline solution and Ti—O of the oxide.

[0018] The water treatment may reduce the ratio of precursor ligand to oxide (precursor ligand:oxide) by at least 20%. The water treatment may reduce the ratio of precursor ligand to oxide (precursor ligand:oxide) by at least 25%.

[0019] It is thus a feature of at least one embodiment of the present invention to remove precursor Cl ligands by causing a reaction between water and the Cl ligands and thus minimizing OH^- permeability.

[0020] The photoanode material may be silicon (Si).

[0021] The thin film of oxide may be TiO_2. The metal precursors may be $TiCl_4$. The remaining precursor ligands may be Cl ligands.

[0022] It is thus a feature of at least one embodiment of the present invention to provide a protection layer promoting chemical stability to the unstable photoanode material.

[0023] The inert gas may be N_2 or Ar.

[0024] It is thus a feature of at least one embodiment of the present invention to expose the substrate to two reactants one at a time to react with the substrate and slowly deposit a thin film of oxide.

[0025] The method may further comprise sputtering nickel (Ni) onto the thin film matrix.

[0026] It is thus a feature of at least one embodiment of the present invention to promote generation of molecular oxygen through a chemical reaction, such as the electrolysis of water into oxygen and hydrogen.

[0027] The step of water pulsing may have a duration of at least 2 hours. The step of water pulsing onto the thin film matrix may be pulsing with a water pulse that is at least 0.5 second and the water pulse is repeated.

[0028] The step of inert gas purging may have a duration of at least 5 hours. The step of inert gas purging onto the thin film matrix may be purging with an inert gas that is at least 0.5 second and the insert gas purge is repeated.

[0029] It is thus a feature of at least one embodiment of the present invention to reduce the amount of remaining precursor ligands in the thin film matrix.

[0030] The temperature of the atomic layer deposition may be at less than or equal to 80 degrees Celsius.

[0031] It is thus a feature of at least one embodiment of the present invention to reduce crystallized particles within the film which contributes to formation of intermediates.

[0032] The temperature of the water treatment may be at less than or equal to 80 degrees Celsius.

[0033] It is thus a feature of at least one embodiment of the present invention to maintain the same temperature and vacuum of the ALD growth chamber when performing the water treatment steps following ALD.

[0034] The thin film of oxide may have a thickness that is less than 15 nm. The thin film matrix may have a thickness that is less than 40 nm.

[0035] It is thus a feature of at least one embodiment of the present invention to minimize crystal formation within the thin film.

[0036] The atomic layer deposition and water treatment may be performed in a vacuum.

[0037] In one embodiment of the present invention, the present invention also provides a photoelectrode comprising: a thin film of oxide deposited onto a photoanode material via atomic layer deposition using a metal precursor reacted with an oxygen precursor (e.g., H_2O, H_2O_2 or O_3) resulting in a precursor ligand wherein the remaining precursor ligand to oxide ratio is less than 3%.

[0038] These particular objects and advantages may apply to only some embodiments falling within the claims and thus do not define the scope of the invention.

BRIEF DESCRIPTION OF THE DRAWINGS

[0039] FIG. **1** is a schematic representation of a Si/TiO_2/Ni photoanode of the present invention for PEC water oxidation having an n-type Si photoabsorber wafer coated with an ultrathin film of amorphous TiO_2 via ALD and further coated with an outer layer of Ni film;

[0040] FIG. **2** is a schematic representation of pinhole formation in Cl-containing amorphous TiO_2 films during PEC water oxidation;

[0041] FIG. **3** is a schematic representation of water treatment of the present invention showing the unreacted Cl ligands in amorphous TiO_2 being removed by reacting with H_2O molecules diffused through the film surface and forming a more continuous, interconnected Ti—O—Ti network;

[0042] FIG. **4** are X-ray photoelectron spectroscopy (XPS) core spectra of (a) Cl 2p where shaded areas are integrated Cl $2p_{1/2}$ and $2p_{3/2}$ peaks where dash lines are baselines for peak area integration and (b) Ti 2p shows an intensity comparison at different binding energies between pristine and water treated TiO_2 thin films;

[0043] FIG. **5** are energy dispersive X-ray spectroscopy (EDS) spectra of pristine and water treated TiO_2 collected from (a) the top and (b) the bottom regions from the cross sections (peaks were normalized by the Ti K peaks) and insets are enlarged Cl peaks showing the intensity change after water treatment where dash lines are baselines for peak area integration;

[0044] FIG. 6 are (a) electrochemical impedance spectroscopy (EIS) measurements of photoanodes protected by pristine and water-treated TiO_2 films under 1 sun illumination and inset is the equivalent circuit for curve fitting; (b) Jph-V curves of Si/TiO2/Ni photoanodes protected by pristine and water treated amorphous TiO_2 films; (c) chronoamperometry of the Si/TiO_2/Ni electrode (with water-treatment) measured in 1.0 M KOH aqueous solution under 1 sun illumination at an external bias of 1.8 V vs. RHE. Dotted line marks 90% of the original Jph value; (d) Jph-V curves of Si/TiO2/Ni photoanode (with water treatment) obtained at a series of time points from the chronoamperometry test; and

[0045] FIG. 7 is a flow chart showing the steps of ALD followed by post-ALD water treatment according to the present invention.

DETAILED DESCRIPTION OF THE PREFERRED EMBODIMENT

[0046] Referring to FIG. **1**, a typical configuration of a Si-based electrode or photoanode **10** is illustrated. The Si-based electrode **10** is composed of a light absorber or photoabsorber **12** of Si photoanode material, coated with an intermediate protective layer **14** of a conformal and pinhole-free inert oxide coating, and further coated with an outer catalyst layer **16** of a metal electrocatalyst coating for efficient oxygen evolution reaction as further described below.

[0047] In one embodiment of the present invention, the photoabsorber **12** is an n-type Si wafer. The outer surface **18** of the photoabsorber **12** experiences rapid corrosion or dissolution in alkaline electrolytes **20**, for example, NaOH or KOH aqueous solution or the like, which leads to instability and high overpotential of the Si-based electrode **10**. To overcome the corrosion or dissolution of the photoabsorber **12**, the photoabsorber **12** is coated with a thin and dense protective layer using high vacuum-based techniques such as atomic layer deposition (ALD).

[0048] The photoabsorber **12** may be coated via ALD with the intermediate protective layer **14** which may be an ultrathin film (e.g., about 24 nm thick or less than 25 nm thick) of amorphous TiO_2. The conformal amorphous TiO_2 protective layer **14** prohibits OH^- group **26** diffusion and thus protects the Si wafer outer surface **18** from chemical corrosion. The amorphous TiO_2 protective layer **14** can also passivate Si wafer surface defect states to suppress charge recombination at the Si—TiO_2 interface. Meanwhile, the amorphous TiO_2 protective layer **14** still permits adequate hole transport **22** through defect band conduction, allowing for unimpaired PEC efficiency.

[0049] Owing to the excellent conformality of ALD, the amorphous TiO_2 protective layer **14** shows an extremely clear and smooth outer surface **24** without any observable particle features. The high homogeneity of the amorphous TiO_2 protective layer **14** without any observable crystalline phases is a desired coating feature that is expected to bring high stability and long lifetime to the Si-based PEC system when submerged in alkaline electrolyte **20**.

[0050] Although protection performance has been shown to be the highest with amorphous TiO_2 and this amorphous TiO_2 protective layer **14** is a preferred embodiment of the present invention, other amorphous ALD oxide films, such as Al_2O_3, HfO_2, and ZrO_2 may be used as the intermediate protective layer **14** in a similar manner to coat and protect the photoabsorber **12**.

[0051] Finally, the amorphous TiO_2 protective layer **14** is coated with an outer catalyst layer **16** of nickel (Ni) metal acting as the oxygen evolution reaction (OER) catalyst. The outer catalyst layer **16** is needed because the oxygen evolution kinetics of Si and TiO_2 are inherently slow. The outer catalyst layer **16** for the OER may be an ultrathin film (e.g., about 12 nm thick or less than 15 nm thick) of Ni metal.

[0052] The Si-based electrode **10** as shown may be denoted as Si/TiO_2/Ni. The Si-based electrode **10** may be the light facing photoanode, however, it is understood that the photoanode and the photocathode may be constructed in a similar manner. It is also understood that the photoabsorber **12**, intermediate protective layer **14**, and outer catalyst layer **16** may be interchanged with other suitable materials. For example, although Si is the preferred photoabsorber **12**, it is understood that other single-crystalline semiconductors may be used such as III-V materials, for example, GaAs, InP, GaN and GaP, or II-VI materials, for example, CuS, CuSb, SnS, in a similar manner. Other outer catalyst layers **16** that can be used include platinum (Pt), ruthenium (Ru) and iridium (Ir) oxides, cobalt phosphate (CoPi), Fe—, Ni—, and Co-based oxides, Fe—, Ni—, and Fe-based (oxy)hydroxides, and the like.

[0053] To improve the lifetime of Si-based electrodes **10** and the surface protection of the intermediate protective layer **14**, i.e., amorphous ALD oxide films, the present inventors have identified the essential structure-property relationships that dictate the protection lifetime control of the intermediate protective layer **14**.

[0054] First, structural inhomogeneity in the intermediate protective layer **14** (e.g., imbedded intermediate phases) may induce highly localized current through the intermediate protective layer **14** and facilitate pinhole formation **28** contributing to intermediate protective layer **14** failure. Therefore, a low-temperature, crystalline-free intermediate protective layer **14** is preferable.

[0055] Second, unreacted precursor ligands and byproducts are another inevitable issue associated with the low temperature ALD processes with depositing the intermediate protective layer **14**. These impurities may substantially change the properties of the intermediate protective layer **14**, such as electronic and ionic transport properties, mechanical stability, and chemical reactivity. Therefore, removing the ligand residues, without introducing any additional crystallization, is preferable.

Example 1: Identifying the Role of Intermediates in the Amorphous Film

Methods

[0056] Atomic layer deposition of TiO_2 on Si substrate: The 380 μm-thick, 3 inch-diameter, single-side polished, <100> oriented, phosphorus doped, n-type Si wafers with resistivity of 1-10 Ω·cm are used for all TiO_2 film deposition and photoelectrochemical (PEC) devices. Wafers are cleaned sequentially in the ultrasonic bath of acetone, isopropanol and deionized (DI) water for 20 min. Prior to TiO_2 depositions, Si wafers are immersed in 5 wt % HF to remove the native oxide. TiO_2 coating is conducted in a homemade atomic layer deposition (ALD) system.

[0057] Specifically, the target substrate is loaded on a quartz tube and placed at a position 5 cm away from the precursor inlet nozzle. N_2 gas with a flow rate of 40 sccm is introduced into the chamber to serve as the carrier gas. The

system's base pressure is kept at 3.8 Torr. The chamber temperature is maintained at 160° C. The deposition temperature is adjusted to 120° C. $TiCl_4$ (Sigma-Aldrich, 99.9%)(i.e., metal precursor) and DI H_2O vapors (i.e., oxygen precursor; can be H_2O, H_2O_2 or O_3) are pulsed into the deposition chamber separately with a pulsing time of 0.5 s and separated by 60 s N_2 purging. Therefore, referring briefly to FIG. **7**, one deposition cycle involves 0.5 s of H_2O pulse+60 s of N_2 purging+0.5 s of $TiCl_4$ pulse+60 s of N_2 purging with a $TiCl_4$ pressure change of 120 millitorr (chamber pressure difference before and after ALD valve open), as seen in steps **50**, **52**, **54**, and **56**, respectively. The chamber is cooled down naturally under N_2 flow after growth. The 24 nm and 2.5 nm-thick TiO_2 coatings are received after 400 and 40 ALD cycles, respectively, corresponding to a growth rate of 0.06 nm per cycle.

[0058] $TiCl_4$ is chosen as the metal precursor, rather than organometallic Ti precursors, since $TiCl_4$ can avoid the involvement of big organic molecules, which may dim the structure and property comparison between intermediates and amorphous/crystalline counterparts. Being free of organic byproducts may improve the accuracy of the observation and analysis of the metastable intermediates. Moreover, metal halide precursors may promote the nucleation of ALD TiO_2 and thereafter enrich the pool of intermediates.

[0059] Sputtering of Ni on TiO2 coated Si: The 12 nm Ni films are deposited on TiO_2 coated Si through sputtering using a CVC 601 DC sputtering system. During the deposition the substrate is rotated at a speed of 5 rpm. The flow rate of argon gas is 25 sccm. The deposition time, pressure, power, voltage, current are: 120 s, 10 militorr, 200 W, ~300 V, ~0.65 A, respectively.

[0060] PEC Electrode fabrication: The back sides of Si wafer are first scratched with a diamond scribe (to remove the native oxides), and then are coated with Ga/In eutectic mixture and connected to a metal lead, forming an Ohmic back contact. Silver paint is then used to affix the lead. After drying in the fume hood, the entire back side and partial front side of the Si electrodes are encapsulated in Epoxy (Loctite, 9460), establishing an exposed active area of ~0.1 cm^2. Calibrated digital images and ImageJ are used to determine the geometrical area of the exposed electrode surface defined by epoxy.

[0061] Electrochemical measurements: The PEC tests are carried out in a typical three-electrode electrochemical setup with Si/TiO2/Ni as the working electrode, a Pt wire as the counter electrode and a Hg/HgO electrode as the reference electrode. The electrolyte is 1 M NaOH aqueous solution. During the cyclic voltammetry (CV) and chronoamperometry scanning, working electrodes are illuminated by a 150 W Xenon lamp coupled with an AM 1.5 global filter with a light intensity of 100 $mW \cdot cm^{-2}$ (one sun). Chronoamperometry curves are measured at a constant external bias of 1.8 V vs. RHE. Hg/HgO is converted to RHE using the following relationship: $E(RHE)=E(Hg/HgO)+0.098\ V+0.059\times pH$. All electrochemical curves are recorded using an Autolab PGSTAT302N station.

[0062] SEM characterizations: Scanning electron microscopy (SEM) images are acquired on a Zeiss LEO 1530 field-emission microscope with a gun voltage of 5 kV and a working distance of ~3 mm. SEM energy dispersive X-ray spectroscopy (EDS) is performed at a voltage of 10 kV and a working distance of ~8 mm. The cross-sectional SEM images are obtained by physically breaking the PEC device and then choosing the piece of wafer with sharp fresh edge. To improve picture quality, the front side of the sample is electrically connected to the SEM stage through a conductive carbon tape.

[0063] AFM measurements: Atomic Force Microscopy (AFM) characterizations are conducted using a XE-70 Park System. For the c-AFM, the 24 and 2.5 nm-thick TiO_2 films are grown on 380 μm-thick, boron heavily doped, single-side polished, <100> oriented, p type wafer with a resistivity of 0.001-0.005 Ω·cm. The Si wafer are then electrically glued onto a steel disc using Ga/In eutectic and silver paste, creating an Ohmic contact between Si and steel disc, similar to the PEC electrode fabrication case. The AFM is operated in contact mode with platinum cantilevers and a complete circuit is formed by AFM tip-TiO_2/Si-AFM stage. The current mappings are recorded under a constant bias of −3 V while the tomography images are probed simultaneously. The individual current-voltage curves are collected by swiping the bias between 3 V to −3 V.

[0064] STEM sample preparation: Cross sectional scanning transmission electron microscopy (STEM) samples are prepared by in-situ lift out using a Zeiss Auriga focused ion beam (FIB). The final FIB milling voltage is reduced to 2 kV to minimize damage from implanted Ga. The final milling is performed on a Fischione 1050 Nano mill equipment with accelerating voltage of 0.5 kV and an incident angle of 10°.

[0065] STEM and EELS observations: STEM and electron energy loss microscopy (EELS) experiments are performed on a FEI Titan microscope with a CEOS probe aberration-corrector operated at 200 keV. The probe semi-angle is 24.5 mrad and the probe current is ~25 pA. The estimated probe size is less than 1 Å. Annular bright field (ABF) STEM image is collected by Gatan 805 BF/DF detector spanning 5.7 to 12.6 mrad. EEL spectrum image is recorded with GIF 865 spectrometer, with energy dispersion of 0.2 eV/pixel, which allowed the simultaneous visualization of the Ti-L and O—K EELS edges. The energy resolution is 0.85 eV measured from the full width at half maximum of zero-loss peak. Quantifications are calculated using the Digital Micrograph implementation of the standard quantification method.

Results

[0066] The structural inhomogeneity in the amorphous TiO_2 thin film (e.g., imbedded intermediate phases) induces highly localized current through the amorphous film and facilitates pinhole formation. When the amorphous TiO_2 thin film is employed for PEC electrode protection, the intermediates raise local concentration of hydroxyls and promote the formation of pinholes through the amorphous matrix.

[0067] One effective kinetic principle to suppress the formation of intermediates is to confine the material to an extremely small volume, which may largely slow down the nucleation rate of a new phase as a result of reduced bulk free energy and limited space for atom rearrangement. This principle is thus implemented in the amorphous TiO_2 thin films to restrict the formation of intermediates by reducing the film thickness to 2.5 nm, while other ALD growth conditions remained identical. For example, reducing the film thickness to 2.5 nm yielded an amorphous thin film with excellent homogeneity. The 2.5 nm protection film accomplished over 500 h electrode longevity at a photocurrent density of ~30 $mA \cdot cm^{-2}$, largely exceeding the stability obtained from the 24 nm TiO_2 protection.

[0068] In addition to film thickness, the deposition temperature is also decreased to 120° C., while other ALD growth conditions remained identical. By decreasing the deposition temperature, the PEC stability increased and had much fewer crystalline particles compared to the control. The presence of highly conductive intermediates also decreased.

[0069] These film thickness and temperature influences further confirmed that kinetics routes of suppressing the formation of intermediates are directly correlated to the protection performance. In addition to the control of film thickness and growth temperature, manipulating other deposition parameters (e.g., Ti precursors, pulse and purge times, and doping) may potentially further improve the protection performance by impeding the formation of intermediates.

[0070] Therefore, a low-temperature crystalline-free amorphous film is preferable for achieving a longer lifetime. This is accomplished by decreasing the film thickness and decreasing the deposition temperature.

Example 2: Identifying the Role of Unreacted Precursor Ligands and Byproducts in the Amorphous Film

Methods

[0071] ALD synthesis of TiO_2 thin films: The n-type Si wafers in the experiments are 380 μm-thick, 3 inch-diameter, single-side polished, <100> oriented, and have a resistivity of 1-10 Ω·cm. Prior to ALD, Si wafers are washed by acetone, isopropanol and deionized (DI) water in an ultrasonic bath for 20 min sequentially, followed by immersing in 5 wt % HF solution to remove the native oxide.

[0072] TiO_2 is deposited in a homemade ALD system. Specifically, N_2 gas with a flow rate of 40 sccm is introduced into the chamber to serve as the carrier gas. The system base pressure is kept at 780 mTorr. The chamber temperature is maintained at 100° C. for depositions. Precursors used for TiO_2 deposition are $TiCl_4$ (Sigma-Aldrich, 99.9%) (i.e., metal precursor) and DI H_2O (i.e., oxygen precursor; can be H_2O, H_2O_2 or O_3). $TiCl_4$ (Sigma-Aldrich, 99.9%). Both precursor vapors are pulsed into the deposition chamber separately with a pulsing time of 0.5 s each and separated by 60 s N_2 purging. Therefore, referring briefly to FIG. **7**, one deposition cycle involves 0.5 s of H_2O pulse+60 s of N_2 purging+0.5 s of $TiCl_4$ pulse+60 s of N_2 purging, as seen in steps **50**, **52**, **54**, and **56**, respectively. Through this procedure, ~15 nm TiO_2 film is obtained after 200 cycles. For TDMAT-TiO_2 film, the film is deposited under recommended temperature of 250° C. in Fiji G2 ALD with TDMAT precursor (Sigma-Aldrich, 99.99%) with 300 cycles for comparison.

[0073] PEC electrode preparation: Ni films are deposited on TiO_2-coated Si by sputtering using a CVC 601 DC sputtering system. The substrate is rotated at a speed of 5 rpm with argon flow at 25 sccm. The deposition is performed under 10 mTorr with 120 s deposition time. Then, the back side of Si wafer is scratched by a diamond scribe and covered by Ga/In eutectic mixture. Silver paste is applied to fix the metal lead to the Ga/In eutectic mixture to achieve good Ohmic contact. After drying in a fume hood, the entire back side and partial front side of the Si/TiO_2/Ni electrodes are encapsulated by Epoxy (Loctite, 9460) with an exposed active area of ~0.05 cm^2. ImageJ is used to determine exposed electrode area.

[0074] Electrochemical characterizations: The PEC tests are carried out in a typical three-electrode electrochemical setup with Si/TiO_2/Ni as working electrode, a Pt wire as counter electrode, and a Hg/HgO electrode as reference electrode. The electrolyte is 1 M KOH aqueous solution. For the cyclic voltammetry (CV) and chronoamperometry measurement, working electrodes are illuminated by a 150 W Xenon lamp coupled with an AM 1.5 global filter with a light intensity of 100 mW·cm−2 (one sun). Chronoamperometry curves are measured at a constant bias of 1.8 V vs. RHE. Electrochemical impedance spectroscopy (EIS) is conducted under open circuit voltage from 100 kHz to 0.1 Hz. All electrochemical curves are recorded using an Autolab PGSTAT101 station.

[0075] Materials characterizations: Scanning electron microscopy (SEM) images are acquired on a Zeiss LEO 1530 field-emission microscope with a gun voltage of 5 kV and a working distance of ~3.5 mm. X-ray photoelectron spectroscopy is acquired by Thermo Scientific K-alpha XPS instrument. Atomic Force Microscopy (AFM) topography is obtained using an XE-70 Park System. Device corrosion area percentages are statistically analyzed by ImageJ. Four dimensional scanning transmission electron microscopy (4D-STEM) is performed using Thermofisher Scientific Themis Z STEM operated at 300 kV and equipped with an Electron Microscopy Pixel Array Detector (EMPAD) to acquire nano-diffraction patterns from different sampling areas within the films. Intensity variance of acquired nano-diffractions are calculated. EDS is performed using FEI Themis Z microscope at 300 kV equipped with 4 Super-X detectors, and the chemical composition of amorphous films is obtained by analyzing EDS spectra using FEI Vlox software and Kα energies for Ti, Cl, and O. The presence of crystalline phases within the amorphous matrix is investigated by observation of the film using low angle annular dark field (LAADF) STEM imaging, including diffraction contrast.

Results

[0076] Chronoamperometry test at a bias of 1.8 V versus reversible hydrogen electrode (RHE) revealed a quick photocurrent density (J_{ph}) decay, where the original value dropped by 10% within just 30 hours. At the point of failure (defined as the time point when J_{ph} reached <90% of its original value), a large number of interconnected pores appeared on the electrode surface, suggesting low stability of this TiO_2 coating. These large pores evolved from small pinholes as early as a few hours of operation, while J_{ph} is still >95% of its original value. The large pores would isolate the Si photoabsorber from Ni catalyst layer and facilitate the formation of insulating SiO_x that limits the hole transport from Si to Ni catalyst. As a result, the Si/TiO_2/Ni photoanode PEC performance is impaired.

[0077] The J_{ph} vs. potential (V) curves are recorded at a few time points through the chronoamperometry test. In the first hour, the water oxidation onset potential is 1.08 V versus RHE and J_{ph} reached a saturated value of 31.5 mA/cm^2 at 1.8 V versus RHE. The saturated J_{ph} and onset potential are on par with reported benchmark n-Si-based photoanodes, indicating the high quality of the Si/TiO_2/Ni system. This onset potential is kept steady for the first 15 hours, but quickly shifted positively to 1.11 V and 1.24 V versus RHE at the 30-hour and 35-hour operation time points, respectively. The higher onset potential implied the

increase of charge transfer resistance in the PEC system, which is typically induced by the formation of insulating SiO_2 layer due to Si corrosion. Accordingly, saturated J_{ph} dropped continuously to 30.2, 29.8, 28.8, and 21.9 mA/cm^2 at the PEC operation time of 5, 15, 30 h, and 35 h respectively, consistent with the decay trend in the stability test. During PEC operation, because no extra redox peaks other than the $Ni(OH)_2$/NiOOH couple are observed from the J_{ph}-V curves, the corrosion of TiO_2 layer is a result of chemical dissolution without valence change.

[0078] The TiO_2-coated Si wafer is immersed in a 1M KOH aqueous solution to evaluate the chemical stability of the amorphous TiO_2 film. Without an external bias, the TiO_2-coated Si wafer still exhibited obvious corrosion but with square-like pores, a typical morphology of chemically corroded Si wafer in alkaline solution. This type of corrosion is also started from pinholes as a result of TiO_2 dissolution confirmed by XPS analyses, suggesting the chemical reactivity of as-deposited TiO_2 would primarily be responsible for the failure.

[0079] Referring to FIG. **2**, the existence of Cl elements may be attributed to the unreacted Cl ligands **30** from the $TiCl_4$ precursor at a relatively low deposition temperature (100° C.). Considering the presence of an appreciable amount of precursor ligand residues (Cl from $TiCl_4$ precursor) in the film, the unreacted Cl ligands **30** act as the terminating point in the Ti—O—Ti network **32**, and thus introduce a more permeable amorphous lattice allowing fast reaction **34** between OH^- groups **26** and Ti—O.

[0080] In addition, DFT calculation revealed that residual Cl ligands may also induce in-gap defect states at the middle of the band gap and shifted Fermi level from 2.71 eV to 4.14 eV closer to conduction band, which can enhance the hole conductivity of the amorphous TiO_2 film. This localized conductivity increase can induce local OH^- accumulation at the electrode surface, resulting in pinhole formation **28**, which facilitates the reaction between OH^- and TiO_2. Together, in the PEC system, Cl residues may enable a faster dissolution of TiO_2 and a rapid diffusion of OH^- to reach the vulnerable Si surface.

[0081] Due to the destructive residual Cl ligands, a longer protection lifetime may be achieved by reducing the residual Cl ligands in amorphous TiO_2 film. Furthermore, no crystallization should be induced, as crystalline phases can introduce structural inhomogeneity and jeopardize the film's lifetime.

Post-ALD In-Situ Water Treatment

[0082] Referring to FIG. **3**, in amorphous TiO_2 films deposited at low temperature, residual ligands are inevitable. Although the present inventors do not wish to be bound by any particular theory, it is believed that their presence may significantly increase the film reactivity in alkaline electrolytes, resulting in pinhole formation and quick dissolution. Removing the residual Cl ligands by completing the reaction with extra water exposure leads to closer-to-ideal stoichiometry of TiO_2 film with improved Ti—O—Ti network continuousness.

[0083] Referring also to FIG. **7**, a post-ALD water treatment procedure has been developed to reduce the residual Cl ligands and maintain amorphous film homogeneity simultaneously. After the regular TiO_2 ALD cycles are completed, the amorphous TiO_2 matrix **40** sample is kept in the growth chamber and subjected to alternating water pulses **42** and inert gas purges **43** under the same low temperature, for example, at less than or equal to 100 degrees Celsius and at less than or equal to 80 degrees Celsius, and in a vacuum chamber. Therefore, one post-ALD water treatment cycle may involve 0.5 s of H_2O pulse+10 s of N_2 purging, as seen in steps **42** and **43**, respectively. Water treatment steps may be completed after 1 cycle to thousands of cycles depending on the length of each water pulse and length of each inert gas purge.

[0084] Each water pulse may be at least 0.5 seconds and at least 1 second and at least 1.5 seconds. The total time for the combined water pulses during the total water treatment may be at least 2 hours and at least 3 hours and 4 hours and at least 5 hours. The water pulse may be pulses of oxygen precursors such as H_2O, H_2O_2 or O_3. Although referred to herein as "water pulses" and "water treatment" it is understood that this may refer to pulsing an oxygen precursor including H_2O_2 or O_3 and not just water.

[0085] Each inert gas purge may be at least 10 seconds and at least 15 seconds and at least 20 seconds. The total time for the combined inert gas purges during the total water treatment may be at least 5 hours and at least 6 hours and at least 7 hours and at least 8 hours. The insert gas may be N_2 or Ar.

[0086] Therefore, post-ALD water treatment may involve repeated cycles of H_2O pulse+inert gas purging+H_2O pulse+ inert gas purging . . . etc. The total water treatment duration (total time for water pulses plus total time for gas purging) may be at least 8 hours and at least 9 hours and at least 10 hours.

[0087] During this treatment, water molecules **44** diffuse into the Ti—O—Ti network **32** of the amorphous TiO_2 matrix **40** and reacts with the dangling unreacted Cl ligands **30**, which raises the film's stoichiometry and improves the Ti—O—Ti network **32** continuity.

[0088] The resulting amorphous TiO_2 matrix **48** following the water treatment is less permeable thus limiting the fast reaction between OH^- and Ti—O. Desirably, the water treatment reduces the amount of unreacted Cl ligands and thus the Cl to Ti (Cl:Ti) ratio is reduced to below 3% and below 2.5% and the Cl to Ti (Cl:Ti) ratio is reduced by at least 1% and by at least 1.5% by the water treatment.

[0089] The amorphous film structure is well retained during this extended ALD process, possibly due to the limited mobility of Ti—O polyhedrons inside the amorphous matrix. When applied as a Si photoanode protection layer, this homogeneous amorphous TiO_2 film exhibits an ultra-stable protection performance in alkaline solution, maintaining a very high saturated J_{ph} at 30 mA/cm^2 for ~600 hours.

[0090] This discovery provides a promising solution to decouple the crystallization from raising the ALD reaction completeness. The amorphous ALD film with controlled stoichiometry may enable an essential manufacturing capability leading the PEC photoelectrodes to meet the industrial standard.

[0091] Therefore, post-ALD water treatment, as further described in the examples below, may at least partially remove the unreacted Cl ligands in ALD amorphous TiO_2 films without introducing additional crystallization, and thereby largely improved the film's lifetime for Si-photoelectrode protection.

Example 3: Reducing Unreacted Precursor Ligands and Byproducts in the Amorphous Film Via Post-ALD Water Treatment

Methods

[0092] Post-ALD water treatment: Immediately after the normal ALD procedure being completed, an additional 2400 water pulses are introduced to the ALD chamber. Each water pulse is separated by 10 s N_2 purging. The other chamber conditions remained the same. After this water treatment procedure is completed, the chamber is cooled down under N_2 flow naturally before the sample is removed.

[0093] Free-standing TiO_2 film preparation: To avoid the strong background signal from Si wafer in STEM nano diffraction, free-standing TiO_2 films are prepared by ALD on a sacrificial PVP (Polyvinylpyrrolidone) layer. 2% PVP aqueous solution is prepared and spin-coated on Si wafer at 3000 rpm for 30 s. PVP-coated Si wafer is used in the ALD synthesis of amorphous TiO_2 films under 100° C. for 200 cycles deposition. Each cycle includes 0.5 s of H_2O pulse+60 s of N_2 purging+0.5 s of $TiCl_4$ pulse+60 s of N_2 purging.

[0094] Accordingly, the additional 2400 cycles of water treatment are conducted after normal growth. After synthesis, samples are immersed in water at room temperature for 2 hours to release the TiO_2 film. The free-standing TiO_2 films are scooped by TEM grids for STEM characterizations.

[0095] Materials characterizations: Scanning electron microscopy (SEM) images are acquired on a Zeiss LEO 1530 field-emission microscope with a gun voltage of 5 kV and a working distance of ~3.5 mm. X-ray photoelectron spectroscopy is acquired by Thermo Scientific K-alpha XPS instrument. Atomic Force Microscopy (AFM) topography is obtained using an XE-70 Park System. Device corrosion area percentages are statistically analyzed by ImageJ. Four dimensional scanning transmission electron microscopy (4D-STEM) is performed using Thermofisher Scientific Themis Z STEM operated at 300 kV and equipped with an Electron Microscopy Pixel Array Detector (EMPAD) to acquire nano-diffraction patterns from different sampling areas within the films. Intensity variance of acquired nano-diffractions are calculated. EDS is performed using FEI Themis Z microscope at 300 kV equipped with 4 Super-X detectors, and the chemical composition of amorphous films is obtained by analyzing EDS spectra using FEI Vlox software and Kα energies for Ti, Cl, and O. The presence of crystalline phases within the amorphous matrix is investigated by observation of film using low angle annular dark field (LAADF) STEM imaging, including diffraction contrast.

[0096] Computational Method: The amorphous TiO_2 structure is obtained through a melt-quenched process using the MA potential. The structure is firstly melted in a NVT ensemble at 5000 K for 50 ps with a timestep of 0.5 fs, and cooled down to 3000 K with a timestep of 0.5 fs and 200 ps simulation time. Next, the model is equilibrated at 3000 K for another 50 ps. Finally, the model is annealed from 3000 K down to 300 K at a cooling step of 1 K/ps, equilibrated at 300 K for 100 ps, and statically optimized to minimal energy to obtain the final quenched atomic structure. The a-TiO_2 model consists of 87 atoms within a cubic box. The density of the structure model is consistent with the typical experimental density value of amorphous TiO_2 at room temperature (3.84 g/cm^3). The electronic property of amorphous TiO_2 with and without Cl ligands is then calculated using density functional theory (DFT) implemented in the Vienna ab initio simulation (VASP) package. The generalized gradient approximation exchange correlation functional Perdew, Burke, and Ernzerhof (PBE) with the Hubbard U correction is applied for the structure optimization and the density of states calculation. The U value of 4.2 eV is applied on Ti atoms. The projector augmented wave method (PAW) is used for the effective potential for all atoms. The PAW potentials used in these calculations have valence electron configurations of $3p^6 4s^2 3d^2$ for Ti, $2s^2 2p^4$ for O, and $3s^2 3p^5$ for Cl. The plane wave cutoff energy of 520 eV is used in all the calculations. The convergence criteria are 10^{-6} eV/cell for electronic self-consistent and 0.05 eV/Å for ionic relaxation, respectively. Tetrahedron method with Blöchl corrections is applied for the density of states calculation.

Results

[0097] The post-ALD water treatment preserves the surface flatness and conformality of the as-deposited TiO_2 film. No additional nanoparticles are observed at the film surface. AFM topography scan revealed that the TiO_2 surface kept the same extremely low roughness of ~0.3 nm.

[0098] Referring to FIG. **4**(*a*), XPS Cl 2p spectra showed an apparent intensity drop of both Cl $2p_{3/2}$ (198.16 eV) and Cl $2p_{1/2}$ (199.82 eV) peaks (corresponding to the Cl—Ti bonding) after water treatment. Referring to FIG. **4**(*b*), the fine Ti 2p spectra of both pristine and water-treated films showed an almost identical shape with the dominating Ti^{4+} chemical state located at 459 eV, implying the water treatment did not change the chemical state of Ti^{4+} cation in the network.

[0099] By integrating the Cl, O, and Ti peaks areas as a half-quantitative analysis, the Cl:Ti ratio is found reduced by 27% (from 0.062 to 0.045), confirming a substantial removal of residual Cl ligands from the amorphous TiO_2 film.

[0100] Four-dimensional scanning electron microscopy (4D-STEM) based characterizations are further used to confirm the elemental and structural change from water treatment. The presence of two burry rings in the averaged nano diffraction patterns revealed that no additional crystallization is induced by the water treatment as compared to the pristine TiO_2 film.

[0101] Diffraction also suggested the existence of the medium-range ordering (MRO) in both TiO_2 amorphous films. MRO refers to the nanoscale volumes with relatively high structural ordering within amorphous materials. Here, the variance (V) of the nano diffraction intensity as a function of reciprocal lattice vector k, V(k) is used to measure the degree of MRO. The magnitude of the peak is related to the degree of structural fluctuation created by the distribution of MRO domains, and the peak position is related to the type of MRO. The broad peak at ~3.0 nm^{-1} indicates the MRO is substantially disordered, confirming the amorphous phase. After water treatment, the broad peak position is retained without shifting, demonstrating that the disordered MRO structure is well maintained. The slightly increased peak intensity may be related to Cl ligand removal.

[0102] Referring to FIG. **5**, the change of Cl distribution is directly visualized using long-time energy dispersive spectroscopy (EDS) Cl mapping acquired from the cross-section of both TiO_2 film samples. Compared to the uniform distribution of Cl signal in the pristine TiO_2 film, the Cl signal in

the water treated TiO_2 film is clearly decreased with a concentration gradient, where the Cl signal is nearly undetectable from the top ~5 nm region. EDS spectrums are then collected to quantify the location-dependent chemical composition change (all peak intensities are normalized by the Ti K peaks for comparison).

[0103] Comparing the water treated TiO_2 film to the pristine TiO_2 film, the Cl:Ti ratio in the bottom region is reduced from 3.86% to 2.41% and in the top region is reduced from 2.46% to 1.81%. These characterizations further confirmed that post-ALD water treatment is able to partially remove residual Cl ligands without introducing additional crystallization to the amorphous ALD TiO_2 films.

[0104] The chemical stability of water treated TiO_2 films is then evaluated by immersing the treated Si/TiO_2 sample in a **1**M KOH aqueous solution without applying any external bias. Compared to pristine TiO_2-coated Si, the density of square-like corrosion spots is substantially reduced from ~300 mm^{-2} to ~30 mm^{-2}, with smaller spot sizes. XPS elemental analysis revealed nearly identical Cl 2p, Ti 2p, and O 1s peak intensities after immersion, indicating that the TiO_2 film after water treatment may be largely preserved when facing alkaline solution.

[0105] Electrochemical impedance spectroscopy (EIS) of Si/TiO_2 electrodes is applied to study the possible TiO_2 film conductivity change induced by Cl removal. The Nyquist plots are fitted based on the equivalent circuit model. The Si/TiO_2 electrodes with and without water treatment showed similar charge transfer resistance at the high-frequency region, suggesting partially removing Cl did not impair the charge transport property of the TiO_2 film.

[0106] The above characterizations confirmed that post-ALD water treatment is able to largely improve the chemical stability and preserve the good electrical conductivity.

[0107] Referring to FIG. **6**, to further evaluate its influences to the PEC performance, the same amount of Ni catalysts is deposited on Si/TiO_2 for water oxidation reaction under the same conditions. The Ja-V curves of $Si/TiO_2/Ni$ photoanodes with and without water treatment exhibited similar onset potential and saturated J_{ph}. The slightly increased slope of the J_{ph}-V curve from the water-treated TiO_2 sample suggests there might be less amount of charge recombination due to the improved charge transport property. With the improved PEC performance, the chronoamperometry test is conducted at an external bias of 1.8 V versus RHE. A stable J_{ph} at ~30 mA/cm^2 is recorded for up to ~600 hours, about one order of magnitude longer than the pristine TiO_2-protected Si photoanodes. J_{ph}-V curves are also recorded at a series of reaction time points to understand the PEC property change during this long operation period. The J_{ph}-V curve maintained an identical shape for the first >100 hours, where the electrode surface is nearly intact showing an extremely high stability. The slope started to show a subtle decrease till ~250 hours. By that time, only a few small pinholes evolved on the electrode surface. As the reaction time extended, the $Ni(OH)_2/Ni(OOH)$ redox peaks and the saturated potential gradually shifted anodically, and the J_{ph}-V curve slope slightly decreased. Both can be attributed to the increase of charge transfer resistance due to the formation of SiO_x on the Si surface. The saturated J_{ph} almost maintained at the same ~30 mA/cm^2 throughout the entire testing period, evidencing the long term high water oxidation performance.

[0108] Owing to the much higher chemical stability of the water treated TiO_2 films, the evolution from several pinholes to large, interconnected pores is substantially suppressed. Therefore, Si photoabsorber and the TiO_2/Ni catalyst layer may still maintain a tight connection and allow nearly impaired charge flow before the formation of large pores. When the photoanode approached its failure point at 600 hours, the J_{ph}-V curve exhibited a drastic anodic shift and the saturated photocurrent density decreased apparently. At this point, large and interconnected pores would be observed on the electrode surface, indicating the water treated TiO_2 film may still share the same failure mechanism as the pristine TiO_2 films.

[0109] The post-ALD water treatment is fundamentally different from other regular approaches to improve the stoichiometry of ALD films. Reducing the residual ligands (i.e., raising the ALD reaction completeness to improve the stoichiometry) and suppressing the crystallization are coupled and anticorrelated in regular ALD processes. For example, extending the length of the ALD water pulse may improve the reaction completeness per cycle. After elongating water pulse time from 0.5 s to 6.5 s, Cl 2p core spectrum showed apparent peak intensity drop, validating the improved ALD reaction completeness.

[0110] However, extending the reaction time may also facilitate surface diffusion of as-deposited species that are loosely bonded to the surface. This may enable the rearrangement of surface atoms and form local nuclei on the surface, which may serve as seeds for TiO_2 to grow into nanoparticles. For example, as-prepared TiO_2 film exhibited a large number of nanoparticles on the surface and the corresponding structure heterogeneity yields an impaired protection performance.

[0111] Similarly, due to the lower energy barrier for nucleating, particularly the intermediate phases of TiO_2 at the active growth surfaces, other regular approaches to achieving complete ALD reactions, such as raising the temperature or introducing plasma, are associated with undesirable crystallization, which also jeopardizes the protection lifetime as earlier research discovered. For example, TiO_2 film deposited under 160° C. yielded a large number of crystalline nanoparticles among the amorphous matrix. The corresponding TiO_2-protected Si photoanode only showed a ~70 h lifetime for PEC operation.

[0112] The critical role of water vapor exposure in the post-ALD treatment is further demonstrated by annealing the pristine TiO_2 films in an N_2 atmosphere or under $TiCl_4$ exposure instead. Annealing TiO_2 films in N_2 atmosphere showed almost the same peak intensity in XPS Cl 2p, Ti 2p core spectrum as compared to pristine TiO_2 film, suggesting the inert gas atmosphere will not change the chemical composition of the ALD film. Thus, the PEC performance of N_2-annealed TiO_2 film had a similar lifetime performance as pristine TiO_2 (10% decay within 29 hours).

[0113] Annealing Si/TiO_2 in $TiCl_4$ atmosphere brought extra Cl impurities to the film and exhibited acute chemical instability. A large amount of corrosion spots emerged after 1 day of immersion. The drastic drop of peak intensity in XPS Cl 2p, Ti 2p, and O 1s spectra demonstrated the quick dissolution of TiO_2 from the film. Correspondingly, $TiCl_4$-treated TiO_2 film showed a very short PEC protection lifetime with 10% photocurrent decay in only 1 hour. These control experiments also proved the critical role of Cl

impurities in determining the chemical stability and protection lifetime of ALD TiO_2 films.

[0114] These results are described in the inventors' publication, Dong, Yutao, et al. "Substantial lifetime enhancement for Si-based photoanodes enabled by amorphous TiO_2 coating with improved stoichiometry." *Nature Communications* 14.1 (2023): 1865, and is hereby incorporated by reference.

[0115] Certain terminology is used herein for purposes of reference only, and thus is not intended to be limiting. For example, terms such as "upper", "lower", "above", and "below" refer to directions in the drawings to which reference is made. Terms such as "front", "back", "rear", "bottom" and "side", describe the orientation of portions of the component within a consistent but arbitrary frame of reference which is made clear by reference to the text and the associated drawings describing the component under discussion. Such terminology may include the words specifically mentioned above, derivatives thereof, and words of similar import. Similarly, the terms "first", "second" and other such numerical terms referring to structures do not imply a sequence or order unless clearly indicated by the context.

[0116] When introducing elements or features of the present disclosure and the exemplary embodiments, the articles "a", "an", "the" and "said" are intended to mean that there are one or more of such elements or features. The terms "comprising", "including" and "having" are intended to be inclusive and mean that there may be additional elements or features other than those specifically noted. It is further to be understood that the method steps, processes, and operations described herein are not to be construed as necessarily requiring their performance in the particular order discussed or illustrated, unless specifically identified as an order of performance. It is also to be understood that additional or alternative steps may be employed.

[0117] It is specifically intended that the present invention not be limited to the embodiments and illustrations contained herein and the claims should be understood to include modified forms of those embodiments including portions of the embodiments and combinations of elements of different embodiments as come within the scope of the following claims. All of the publications described herein, including patents and non-patent publications, are hereby incorporated herein by reference in their entireties.

[0118] To aid the Patent Office and any readers of any patent issued on this application in interpreting the claims appended hereto, applicants wish to note that they do not intend any of the appended claims or claim elements to invoke 35 U.S.C. 112(f) unless the words "means for" or "step for" are explicitly used in the particular claim.

What we claim is:

1. A method of removing precursor ligands and byproducts in a photoelectrode, the method comprising:

(a) performing an atomic layer deposition of an oxide onto a photoanode material including the steps of:

pulsing oxygen precursors onto a photoanode material surface;

purging the photoanode material surface with an inert gas;

pulsing metal precursors onto the photoanode material surface; and

purging the photoanode material surface with the inert gas

to deposit a thin film of oxide onto the photoanode material surface to produce a thin film matrix;

(b) performing a water treatment of the thin film matrix including the steps of:

pulsing the oxygen precursors onto the thin film matrix; and

purging the thin film matrix with the inert gas;

to reduce a ratio of precursor ligand to oxide from the thin film matrix.

2. The method of claim **1** wherein the water treatment reduces the ratio of precursor ligand to oxide by at least 20%.

3. The method of claim **2** wherein the water treatment reduces the ratio of precursor ligand to oxide by at least 25%.

4. The method of claim **1** wherein the photoanode material is silicon.

5. The method of claim **1** wherein the thin film of oxide is TiO_2.

6. The method of claim **5** wherein the metal precursors are $TiCl_4$.

7. The method of claim **6** wherein the precursor ligands are Cl ligands.

8. The method of claim **7** wherein the inert gas is N_2 or Ar.

9. The method of claim **1** further comprising sputtering nickel (Ni) onto the thin film matrix.

10. The method of claim **1** where the step of water pulsing has a duration of at least 2 hours.

11. The method of claim **10** wherein the step of water pulsing onto the thin film matrix is pulsing a water pulse that is at least 0.5 second and the water pulse is repeated.

12. The method of claim **1** wherein the step of inert gas purging has a duration of at least 5 hours.

13. The method of claim **12** where the step of inert gas purging onto the thin film matrix is purging with an inert gas at least 0.5 second and the insert gas purging is repeated.

14. The method of claim **1** wherein the temperature of the atomic layer deposition is at less than or equal to 80 degrees Celsius.

15. The method of claim **1** wherein the temperature of the water treatment is at less than or equal to 80 degrees Celsius.

16. The method of claim **1** wherein the thin film of oxide has a thickness that is less than 15 nm.

17. The method of claim **1** wherein the thin film matrix has a thickness that is less than 40 nm.

18. The method of claim **1** wherein the atomic layer deposition and water treatment are performed in a vacuum.

19. A photoelectrode comprising:

a thin film of oxide deposited onto a photoanode material via atomic layer deposition using a metal precursor reacted with an oxygen precursor resulting in a precursor ligand;

wherein the precursor ligand to oxide ratio is less than 3%.

20. The photoelectrode of claim **19** wherein the photoanode material is silicon and the thin film of oxide is TiO_2.

* * * * *